ISSN: 2640-5571

Reaserch article

Advances in Nanoscience and Nanotechnology

Improvement Physical Features Composite Comprise of Strain Nano-metals (Ag, MN) Assembled on Graphene Suspended Inside PEG Matrix and Its Application

Ameen Abdelrahman*[1], Fouad Erchiqui[2], B M Nedil[2]

[1]*Mechanical Engineering Département, Université du Québec en Abitibi-Témiscamingue (UQAT),445 Boulevard de l'Université Rouyn-Noranda (QC) J9X 5E4.*

[2]*Professeure- d'université | UQAT - Université du Québec en Abitibi-Témiscamingue 445 boul. de l'Université Rouyn-Noranda J9X 5E4 819 762-0971*

***Corresponding author**

Ameen Abdelrahman, Mechanical Engineering Département, Université du Québec en Abitibi-Témiscamingue (UQAT),445 Boulevard de l'Université Rouyn-Noranda (QC) J9X 5E4

Submitted: 08 Nov 2021; **Accepted:** 15 Nov 2021; **Published:** 22 Nov 2021

Citation: *Ameen Abdelrahman, Fouad Erchiqui, B M Nedil (2021) Improvement Physical Features Composite Comprise of Strain Nano-metals (Ag, MN) Assembled on Graphene Suspended Inside PEG Matrix and Its Application. Adv Nanoscie Nanotec 5(1): 28-34.*

Abstract

In order to get desirable flexible conductive and stretchable materials used as future conductive Devices It should find a pathway or create a new composite that is thermally stable, non-toxic, environmentally inexpensive, easier carrier, and highly efficient. The composite chip is composed of metals nanoparticles (MN, Ag), assembled on a thin layer of Nano Graphene impregnated inside the polyethylene glycol (PEG) matrix. Various characterization had been conducted to demonstrate the physical feature of the new composite, like UV, CVT, TEM, XRD, and TGA.

Keywords: Assemble Nano Metals (Ag, MN), Graphene, Polyethylene Glycol (Peg), Conductive

Introduction

Nobody can deny nanocomposite materials has superb performance in different aspect of field life applications especially attention to the industrial part. Like its ability to be permeable and selective for gas/liquid separation, engineering resins, mechanical toughness, and photoconductivity for electronics [1-3]. There is the great compatibility between inorganic nanoparticles Nano filler and the polymer as a matrix to form nanocomposite materials [4]. Many investigated and studies have been conducted on different types of organic polymers that created as matrices to form nanocomposites with many nanoparticles such as titanium, silica, carbon nanotubes, zirconia, and graphene [5-10]. By taking a look at ethylene glycol that has numerous properties such as it is a polarity, economic value, non-expensive, non-toxic high chemical, and thermal stability whatever the useful time is long and no super cooling [11, 12]. Nanoparticles provide us with different Applications and effective ways for improving characteristics of fluid pneumonia [13, 14]. As innovation research graphene and nitrogen-doped has appeared as an attractive applicant for energy transport due to their distinctive structure and properties [15-18].

Referring to covalent functionalization's, whilst Paredes et al [19]. Reveal a good dispersal of graphene oxide (GO) can be acquired not only in water but also in different organic solvents like ethylene glycol, by using an acid treatment which leads to the formation of disorder sites inside the systematically arranged Nano sheets conjugated graphene [20-21].

One of the studies worked on, CuO Nano fluids by the prepared physical [22]. Nonmetal CuO nanoparticles were produced by a physical vapor synthesis method. The CuO powders were then distributed in ethylene glycol base fluid. by measuring the size of CuO particle was 29 nm. Another MWNTs Nano fluids [23].

The relationship between electrical conductivity and the degree of dispersion of Nano fluid approached in previous literature through their experiments, for instance, Ganguly et al [25, 26]. Determined the dynamic electrical conductivity of aqueous Al2O3 and show the variation relation between that properties and temperature with volume fraction. Konakanchi et al [27]. Confirmed the relationship between conductivity on temperature and volumetric concentration by preparing solution from Al2O3, SiO2, and ZnO nanoparticles dissipated in propylene glycol/water solution. several experiments and research uses metals oxides nanoparticles in different base fluids e.g. graphene, Pd in water, Pd/Ag in ethylene glycol and distilled water, and TiO2 in ethylene glycol [28-32].

There is another way to increase the ionic conductivity of polymer electrolytes. This is to focus on increasing ionic dissociation by placing polar subunits, such as acrylamide, acrylonitrile, maleic anhydride, and carbonate, along the chains to increase the polymer host dielectric constant. The polar subunits also help reduce

the crystallinity. The most recent example of this approach is that of Forsyth et al [14]. Who introduced single carbonate groups -[O-C(dO)-O]- into the polyether chain.

In that case, we add some surfactant emulsifier which decreases the surface tension interactions between graphene nanostructures and aqueous/organic solvents addition also using a hydrophilic agent that works on energy features such as edges of graphene Nano sheets) functionalization's [32]. many previous kinds of literature approached water/ ethylene glycol-based Nano fluids, the surfactants. For non-covalent options are sodium dodecyl benzene sulphonate (SDBS), gum Arabic [33, 37], and polyvinyl alcohol (PVA) [38]. The most common methods by using the Hummers method or modifications dependable on the oxidation process and covalent functionalization's [39-42].

Malavasi et al. mentioned that nanoscale material shows important side effects in their reaction mechanism because it has a short diffusion length and large density of molecule interfaces, Eventually, it is considered good evidence to justify the effective nanomaterial commended and the grain boundary interfaces [44, 45]

Experimental Section

2.1. Materials.

Metals Oxides and organic solvents were purchased from Sigma –Aldrich (Toronto, Canada), Graphene Nano powders (purity > 99%, 300 mesh) were bought from Sigma –Aldrich Co. Ltd. (Canada). Most of the Nano metals and other salts (Magnesium oxide, silver acetate, and silver nitrate (purity > 99%,)) were delivered by a scientific fisher, Canada used, n-Hexane, THF was purchased from Sigma Aldrich, Canada.

2.2 Methods

2.2.2 XRD analysis

The MnO2 filter is transferred to RETSCH Planetary Ball Mills Type PM 400, then crushed using the ball mill at speed 150 rpm for 5 h to get Nano size structure, then prepared samples were carried out using X-ray diffraction patterns. It's a Pan Analytical Model X' Pert Pro, which was outfit with CuK α works at radiation (λ = 0.1542 nm), Ni-filter associated with the detector. The diffract grams were investigated at a 2θ range of 0.5°–90° and size of 0.02 Å. All measurements were conducted at All test has been carried out ETS, Montreal.

2.2.3 TEM characterize

All samples characterized were carried out using Transmission electron microscopy (TEM) Model: JEOL JEM-1230 operating at 120 kV associated specifically a CCD camera. All test has been carried out Nano-QAM, Montreal Canada. Measurements of samples conducts were done using a convenient method of prepared samples to get good results throughout the TEM image utilizing copper grids on an amorphous carbon film.

2.2.4 Particle Size Analyzer

Particle analysis has been investigated at Cairo university using Zetasizer Nano S90 (Malvern) modal Nano S90. It is run by Red laser as a Zetasizer instrument at a 90° angle. The test has been carried out in Nano-QAM, Montreal.

2.2.5 Prepared samples of suspended Nanoparticles had been characterized using Ultraviolet-visible (model UV-1800 Shimadzu UV spectrophotometer). The spectral analysis for silver and Manganese samples is investigated around a wavelength of 150 e was 1000 nm.

Results and Discussion.

3.1 Physical properties of composite constituents

Crystalline graphic structure of both Prepared MnO2 and Ag NPs have been investigated by X-ray diffraction, as reported in Fig. 1. This figure illustrates ranges of diffracted intensities registered at 20 matches to planes of (1 1 1), (2 0 0), (2 2 0), and (3 1 1) respectively. These clear out the cubic crystal structure of silver, whose corresponding (d calculated) values are 2.336, 1.955, 1.436, and 1.224 Å for (1 1 1), (2 0 0), (2 2 0), and (3 1 1) planes respectively, as seen below in the same figure Moreover, they coincide with standard silver values using the Debye–Scherrer formula: [1]

$$D = \frac{k\lambda}{\beta \cos \theta}$$

The silver nanoparticles crystallite calculated is ~25 nm, confirmed by using the TEM characterize in Fig. 3. On the other hand, the recorded peak positions (2θ, degree) of Mn-NPS are 18.18, 37.48, 42.82, 58.81, 6.21, 74.58, and 78.43 respectively. The average crystalline size calculated using the Debye-Scherer formula is about 25–30 nm.

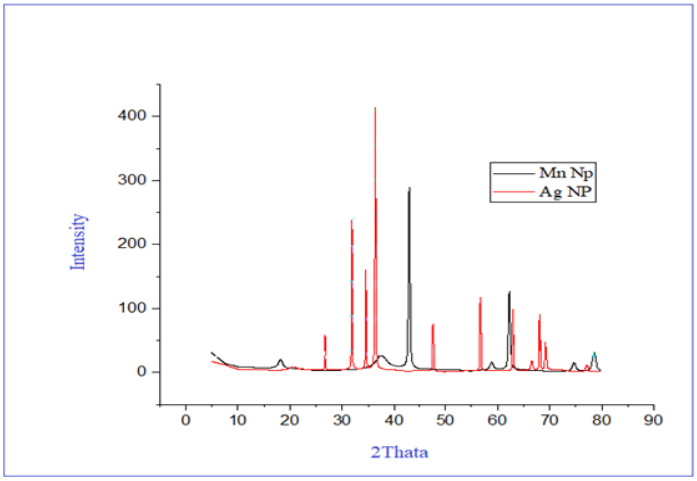

Figure 1: XRD patterns of Mn and Ag nanoparticles.

The TEM image (Figs. 3a, b) shows the average size of both Manganese and Silver particles is 25–30 nm. The Graphene surface sheet contains spread large numbers of Mn nanoparticles demonstrated in Fig 2a, which is based on electronic configuration half fill d-orbitals. These facilitate electron transfer related to oxidation-reduction on the surface of graphene. Another observation is the presence of some floccules and aggregates that appear in Fig. 2a. These could be the immobilization and deposition of Manganese oxide on Graphene surface, or metallic conjugated bonds between Mn+//Mn+2 and Ag+// Ag-, as shown in Fig. 2d.

Suspended graphene particles disperse in polyethylene Glycol as

demonstrated in Fig. 2c. The average size of a particle is 110 to 440 nm. Variety of particle size is due to the aggregation and flocculation of the same units of the same graphene. Furthermore, the viscosity of polyethylene Glycol affected particles volume. With regard to Fig. 2d describes surface morphology of novel composite; there is a complete distribution of numerous of nanoparticles (Mn, Ag, and Graphene) inside PEG matrix of different sizes around 10–30 nm-1, in addition to the flocculation and deposition of particles on the surface of PEG. Particles deposition is the return of interaction forces, spaceman spherical, and viscous nature of a solution. [46]

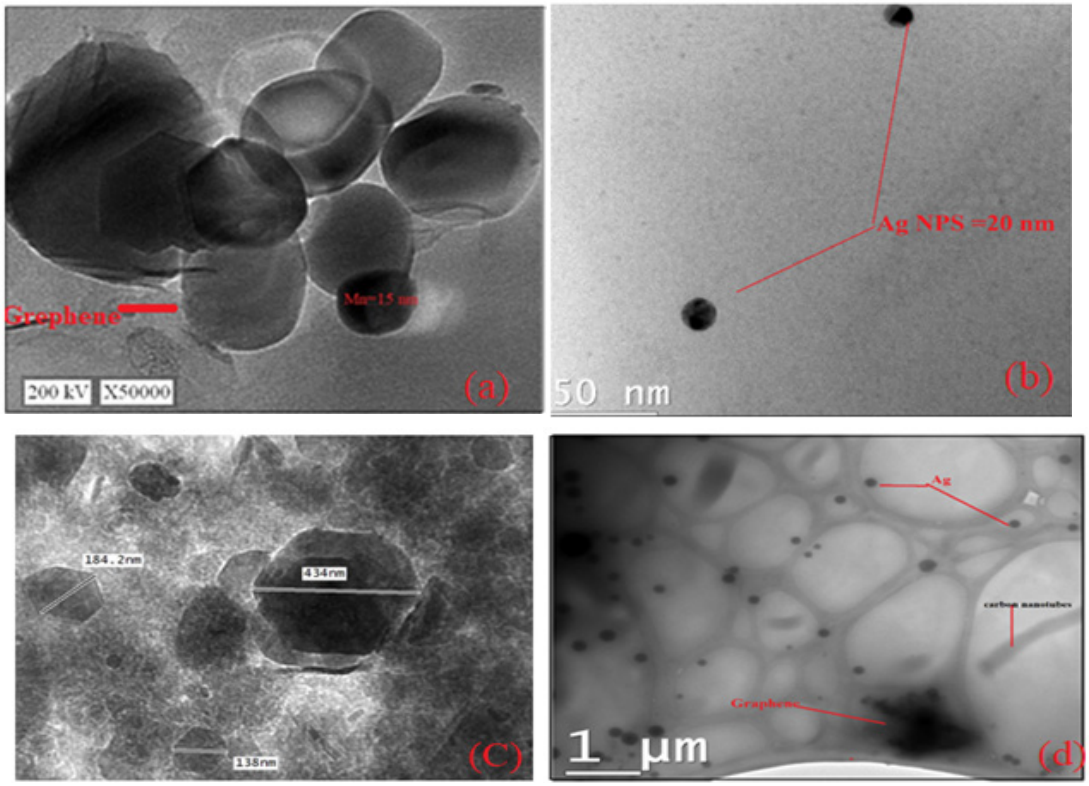

Figure 2: TEM images of: (a) graphene with Mn NPs, (b) Ag NPs in PEG, (c) graphene inside PEG, and (d) PEG–NPs–graphene composite.

3.2 Composite Thermal analysis.

Figure 4a illustrates HDPE decomposition at a flow rate of 10°C/min. A PEHD sample was carried out using a thermal gravimetric analyzer (TGA). Fig. 3b points out the change in the mass fraction of the sample with a function of temperature at different heating rates. Heating rates range from 400 to 520ºC, which shows how similar behavior can be within a single mass loss zone. The degradation zone is approximately centered at 425, 450, and 460ºC at a heating rate of 10°C/min. The temperature reforming zone of HDPE ranges between 380–510ºC. Major mass loss in that stage relates to the elements of CO_2, water, H_2, and light components molecules breakdown of the polymeric chain.

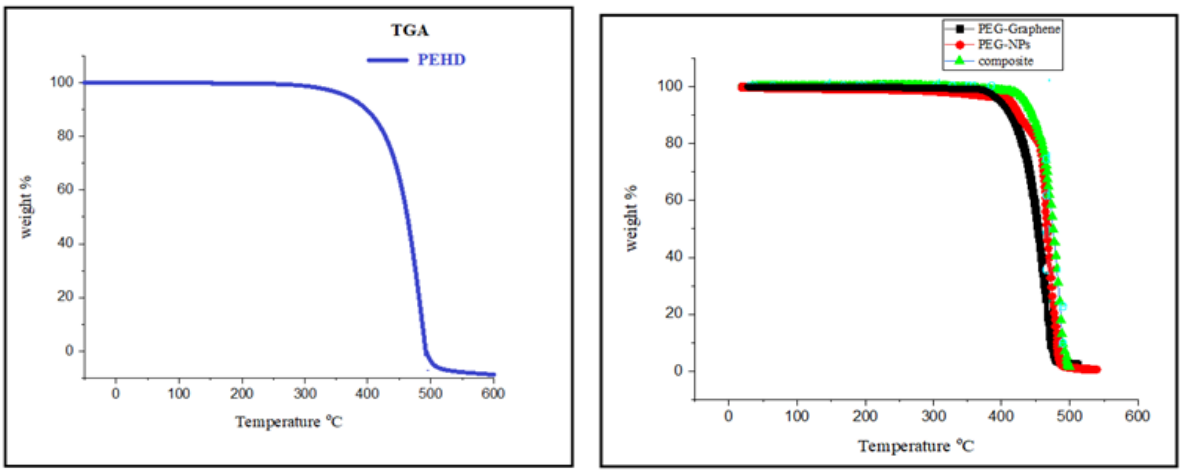

Figure 3: TGA curves for (a) HDPE and (b) composite structure.

On the other hand, though PEG thermal degradation starts low, from 100 to 390°C, losing some molecules like CO2 or water causes only a slight change in its appearance. But in the case of PEG-graphene, the TGA has become higher and requires more heat to dissociate and reach 410°C. This is lower compared with PEG-NPS in Fig. 3b, whose degradation point is 425°C. In consequence, we prepared composites with degradation at 460°C. Also, it is confirmed that Nano metals (Ag and Mn) filled out interspace and irregularly distributed voids of PEG. This leads to a decreased molecular weight and an increased melting point of composites. Furthermore, the TGA of the prepared composite is closer to the temperature of the fixed bed reactor, which was confirmed by another characterization such as EDX and TEM.

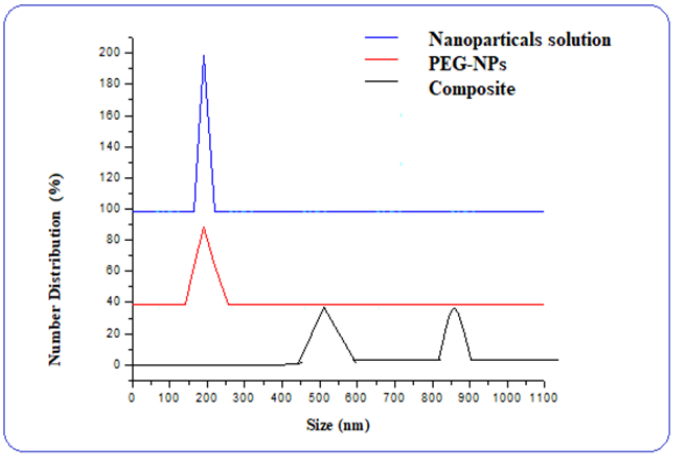

Figure 4: Particle size distributions for (1) suspension of (Mn, Ag) NPs, (2) (Ag, Mn)NPs in PEG, and (3) PEG–(Ag, Mn) NPs–graphene colloid.

Figure 4 illustrates the suspended particles in liquid phases. That technique shows the qualities and quantitative analysis used to investigate particle size and shape. The same figure explains different size particles for different prepared solutions. We have three solutions containing (Magnesium, and sliver) nanoparticles solution, graphene suspended in (Ag, MN) nanoparticles solution, and a mixture of composites (Ag, MN, Graphene, and PEG). We recorded a strong peak in a nanoparticles solution that appears at 110 nm, which is lower than in PEG solution, and composite 220, and 590, 890 d nm respectively. Our interpretation is that the force interaction (shear strength results from PEG apparent viscosity, coated the entire Nano metals particles and different conjugated bonds between nanoparticles together cause massive particles. PEG viscosity has an effecting factor on particle movement and increasing enhancement cross-linked inside a matrix, due to the stability of the composite during thermal degradation.

Absorption spectra

We used UV to illustrate the different signals and spectra of prepared samples. We have three samples: solution of PEG/Metals NPS, PEG/Graphene, and matrix of their solution prepared as shown in Fig. 5. Comparing different curves, we found specific spectra characterizing Ag, whose absorbance slightly shifted at 430 nm due to cross-links with polyethylene glycol through a hydrogen bond. Besides, the graphene in the second curve, which is also shifted, could be the resonance of bi bonds in addition to the contact with polyethylene glycol. The UV-Vis spectrum for this (PEG/graphene /Metals NPS) composite disappeared with the existence of a wide board peak, it could be surface Plasmon resonance of spherical nanoparticles nature, or metallic bonds created between Mn-Ag. That shift is represented in Fig. 5 at 410 and 450 nm. That is good evidence that indicates all nanoparticles (Mn, Ag, and graphene) assembled and impregnated inside the PEG matrix [47,48].

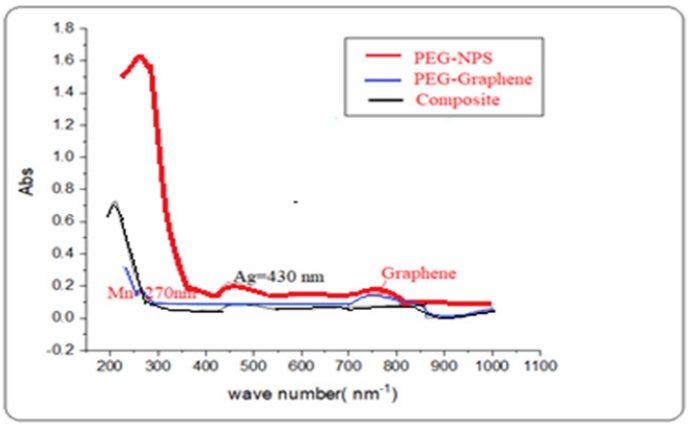

Figure 5. Absorption spectra of (1) suspension of Mn NPs, (2) suspension of Ag NPs, and (3) Graphene.\

3.3. Electrochemical analysis

Cyclic voltammetry (CV) is one of the most important techniques used to measure the rate of oxidation and reduction reaction species in the prepared solution. To conduct that experiment, we need to set up three cell electrodes, and reference, working, and counter electrodes to measure variation change between current and volts. We found a difference in current based on the change of reaction metals (Sliver and Manganese metals). Figure 6 shows different potential states released from the electrochemical series of metals nanoparticles. A slight peak appears at cycle voltammetry curve (-V) 1.2, and (+V) 1.2; it is due to reversible reaction occurred: according to the previous equation Mn+2, oxidase to be Mn0 to give a pair of electrons, on the other side and Ag is gain an electron to be a reducing agent (reversible reaction). That appears in Fig. 6 at electrochemical potential equal (+1.6) V. In conclusion, there are Nemours ions charge transfer through a solution, but on the other hand, the transfer is demolished due to high viscosity of the polymer, which restricts that ions transfer, although it is a protonic solution, and many interface interactions dependable on and van der Waals force mechanism.

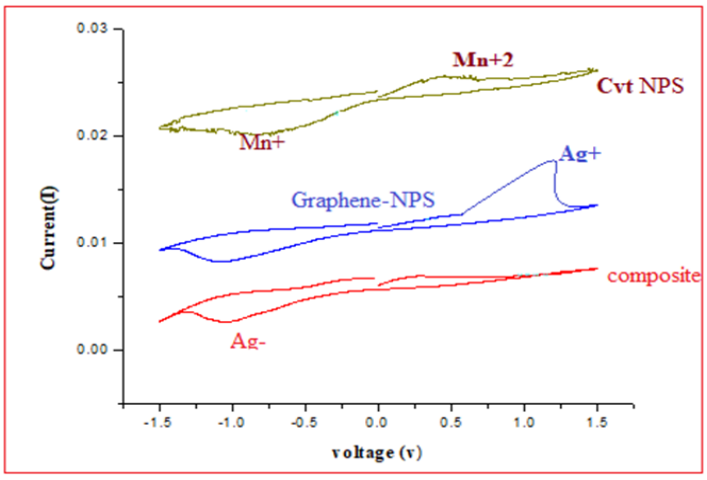

Figure 6: Reaction mechanism as estimated using CVT

Throughout the Cyclic voltammetry (CV) analysis, we concluded that there are various electrochemical reactions occurring between different species of chemical reactions. For instance, Mn has a different (+2, +3, and + 5) valence oxidation state to reach a stable (half or empty) state in the electronic configuration of (d-orbital); therefore, it has a tendency to lose pairs of electrons, which reduces sliver metals and creates serious electrochemical reaction mechanisms. Graphene works as a bridge to transfer the charge between both metal's sides. Due to π-π bonds of graphene structure, which lead to electron resonance and reaction stability, our investigation follows Eq. (1):

Standard cell potential for an electrochemical cell with the following reactions

$$E^{o}_{cell} = E^{o}_{red} + E^{o}ox \qquad (2)$$

Half-reaction mechanism for each process

$$Mn(s) \rightarrow Mn^{2+}(aq) + 2e^{-} \qquad E° = +0.8\ V$$

$$Ag^{+}(aq) + e^{-} \rightarrow Ag(s) \qquad E° = +0.8\ V$$

$$Mn^{2+}(aq) + 2e^{-} \rightarrow Mn(s) \qquad E° = -1.18$$

$$Ag(s) + Mn^{2+}(aq) \leftrightarrow Ag^{+}(aq) + Mn(s)$$

Ag(s) is formed at the cathode while Mn^{2+}(aq), at the anode.
In the latter reaction, Graphene acts as a bridge (electrolyte membrane) [49].

The storage charge is based either on the adsorption of cations at the surface of the electrode material or on the intercalation of cations in their bulk. One of the important values to using Ag as a supported catalyst is its nature and activity as a reducing agent. It has a great effect on free energy according to equation $\Delta G = \Delta H - T\Delta S$, then that reaction will shift to products and become the exothermal reaction. Moreover, it employs an accelerator for the reaction (between graphene surface assembled Mn NPS as the active species and plastic PE). It is due to the down heating rate of reaction during the decomposition process. On the other hand, the average size of Mn and Ag NPs is down 30 nm. The tiny size of Nano metals causes the disorder dispersal on the Graphene surface to make chelating complex then immersed inside PEG matrix. Thus there were created many active sites were, which accelerated the reaction (reducing both reaction time and heating rate of the cracking process). Complete cracking was performed at 600°C instead of 750°C without the catalyst additive.

Conclusion

Organic and inorganic nanocomposite materials play important roles in modern life. For example, nanoparticles or nanowires are mostly used in biological sensors to magnify their applications through nanowire electrical conductivity, electronic configuration, or modified way of nature. Nanoparticle complexes interact with matter. In that paper we reach out to create a novel composite that will be future applicable, that composite has been evaluated and estimated using different characterization to get desirable picking chap [50].

References

1. Peng G, Qiu F, Ginzburg VV, Jasnow D, Balazs AC (2000) Forming Supramolecular Networks from Nanoscale Rods in Binary, Phase-Separating Mixtures. Science 288: 1802-1804.
2. Merkel TC, Freeman BD, Spontak RJ, He Z, Pinnau I, et al. (2002) Ultra Permeable, Reverse-Selective Nanocomposite Membranes. Science 296: 519-522.
3. Wang Y, Herron N (1996) X-Ray Photoconductive Nanocomposites. Science 273: 632-634.
4. He J, Shen Y, Evans DG, Duan X (2006) Tailoring The Performance of Polymer Composites Via Altering the Properties of the Intrapore Polymers of Mcm-48 Nanocomposites as Fillers. Applied Science and Manufacturing 37: 379-384.
5. McCarthy DW, Mark JE, Clarson SJ, Schaefer DW (1998) Synthesis, structure, and properties of hybrid organic–inorganic composites based on polysiloxanes. II. Comparisons between poly (methylphenylsiloxane) and poly (dimethylsiloxane), and between titania and silica. Journal of Polymer Science Part B: Polymer Physics 36: 1191-1200.
6. Motomatsu M, Takahashi T, Nie HY, Mizutani W, Tokumoto H (1997) Microstructure Study of Acrylic Polymer-Silica Nanocomposite Surface by Scanning Force Microscopy. Polymer 38: 177-182.
7. Canché-Escamilla G, Duarte-Aranda S, Toledano M (2014) Synthesis and Characterization of Hybrid Silica/Pmma Nanoparticles and Their Use as Filler in Dental Composites. Materials Science and Engineering 42 : 161-167.
8. Zendehnam A, Mokhtari S, Hosseini SM, Rabieyan M (2014) Fabrication of Novel Heterogeneous Cation Exchange Membrane by Use of Synthesized Carbon Nanotubes-Co-Copper Nanolayer Composite Nanoparticles: Characterization, Performance in Desalination. Desalination 347: 86-93.
9. Kompany K, Mirza EH, Hosseini S, Pingguan Murphy B, Djordjevic I (2014) Polyoctanediol Citrate–Zno Composite Films: Preparation, Characterization and Release Kinetics of Nanoparticles from Polymer Matrix. Materials Letters 126: 165-168.
10. Abu-Zied BM, Hussein MA, Asiri AM (2015) Characterization, In Situ Electrical Conductivity and Thermal Behavior of Immobilized Peg on Mcm-41. International Journal of Electrochemical Science 10: 4873-4887.
11. Pielichowski K, Flejtuch K (2002) Differential Scanning Calorimetry Studies On Poly (Ethylene Glycol) With Different Molecular Weights for Thermal Energy Storage Materials. Polymers for Advanced Technologies 13: 690-696.
12. Alkan C, Sari A, Uzun O (2006) Poly (Ethylene Glycol)/ Acrylic Polymer Blends for Latent Heat Thermal Energy Storage. AIChE journal 52: 3310-3314.
13. Amiri A, Shanbedi M, Chew BT, Kazi SN, Solangi KH (2016) Toward Improved Engine Performance with Crumpled Nitrogen-Doped Graphene Based Water–Ethylene Glycol Coolant. Chemical Engineering Journal 289: 583-595.
14. Amiri A, Shanbedi M, Ahmadi G, Rozali S (2017) Transformer Oils-Based Graphene Quantum Dots Nanofluid as A New Generation of Highly Conductive and Stable Coolant. International Communications in Heat and Mass Transfer 83: 40-47.
15. Luican A, Li G, Reina A, Kong J, Nair RR, et al. (2011) Single-Layer Behavior and Its Breakdown in Twisted Graphene Layers. Physical Review Letters 106: 126802.
16. Amiri A, Ahmadi G, Shanbedi M, Savari M, Kazi SN, et al. (2015) Microwave-Assisted Synthesis of Highly-Crumpled, Few-Layered Graphene and Nitrogen-Doped Graphene for Use as High-Performance Electrodes in Capacitive Deionization. Scientific Reports 5: 1-13.
17. Geim AK, Novoselov KS (2007) The rise of graphene. Nat Mater 6(3): 183-191
18. Li H, Zou L, Pan L, Sun Z (2010) Novel Graphene-Like Electrodes for Capacitive Deionization. Environmental Science & Technology 44: 8692-8697.
19. Paredes JI, Villar Rodil S, Martínez Alonso A, Tascon JMD (2008) Graphene Oxide Dispersions in Organic Solvents. Langmuir 24: 10560-10564.
20. Pop E, Varshney V, Roy AK (2012) Thermal Properties of Graphene: Fundamentals and Applications. MRS bulletin 37: 1273-1281.
21. Teng CC, Ma CCM, Lu CH, Yang SY, Lee SH, et al. (2011) Thermal Conductivity and Structure of Non-Covalent Functionalized Graphene/Epoxy Composites. Carbon 49: 5107-5116.
22. Rasheed AK, Khalid M, Rashmi W, Gupta TCSM, Chan A (2016) Graphene Based Nanofluids and Nanolubricants-Review of Recent Developments. Renewable and Sustainable Energy Reviews 63: 46-362.
23. Liu MS, Lin MC, Huang IT, Wang CC (2006) Enhancement of Thermal Conductivity with Cuo for Nano fluids. Chemical Engineering & Technology: Industrial Chemistry-Plant Equipment-Process Engineering-Biotechnology 29: 72-77.
24. Liu MS, Lin MCC, Huang IT, Wang CC (2005) Enhancement of Thermal Conductivity with Carbon Nanotube for Nano fluids. International Communications in Heat and Mass Transfer 32: 1202-1210.
25. Wang R, Billone PS, Mullett WM (2013) Nano Medicine in Action: An Overview of Cancer Nano medicine On the Market and in Clinical Trials. Journal of Nanomaterials 2013.
26. Ganguly S, Sikdar S, Basu S (2009) Experimental Investigation of the Effective Electrical Conductivity of Aluminum Oxide Nano fluids. Powder Technology 196: 326-330.
27. Konakanchi H, Vajjha R, Misra D, Das D (2011) Electrical Conductivity Measurements of Nanofluids and Development of New Correlations. Journal of Nanoscience and Nanotechnology 11: 6788-6795.
28. Kole M, Dey TK (2013) Investigation of Thermal Conductivity, Viscosity, and Electrical Conductivity of Graphene Based Nano fluids. Journal of Applied Physics 113: 084307.
29. Goharshadi EK, Azizi Toupkanloo H, Karimi M (2015) Electrical Conductivity of Water-Based Palladium Nano Fluids. Microfluidics and Nano fluidics 18: 667-672.
30. Azizi Toupkanloo H, Goharshadi EK, Nancarrow P (2014) Structural, Electrical, and Rheological Properties of Palladium/Silver Bimetallic Nanoparticles Prepared by Conventional and Ultrasonic-Assisted Reduction Methods. Advanced Powder Technology 25: 801-810.
31. Minea AA, Lorenzini G (2017) A Numerical Study on ZnO Based Nano fluids Behavior on Natural Convection. International Journal of Heat and Mass Transfer 114: 286-296.
32. Amiri A, Sadri R, Shanbedi M, Ahmadi G, Chew BT, et al.

(2015) Performance Dependence of Thermosyphon On the Functionalization Approaches: An Experimental Study On Thermo-Physical Properties of Graphene Nano Platelet-Based Water Nano fluids. Energy Conversion and Management 92: 322-330.
33. Kazi SN, Badarudin A, Zubir MNM, Ming HN, Misran M, et al. (2015) Investigation on the Use of Graphene Oxide as Novel Surfactant to Stabilize Weakly Charged Graphene Nano platelets. Nanoscale Research Letters 10: 1-15.
34. Li X, Chen Y, Mo S, Jia L, Shao X (2014) Effect of Surface Modification on the Stability and Thermal Conductivity of Water-Based Sio2-Coated Graphene Nano fluid. Thermochim Acta 595: 6-10.
35. Sadeghinezhad E, Mehrali M, Saidur R, Mehrali M, Latibari ST, et al. (2016) A Comprehensive Review On Graphene Nanofluids: Recent Research, Development and Applications. Energy Conversion and Management 111: 466-487.
36. Yu W, Xie H, Wang X, Wang X (2011) Significant Thermal Conductivity Enhancement for Nano fluids Containing Graphene Nano sheets. Physics Letters A 375: 1323-1328.
37. Ahammed N, Asirvatham LG, Wongwises S (2016) Effect of Volume Concentration and Temperature On Viscosity and Surface Tension of Graphene-water Nano fluid for Heat Transfer Applications. Journal of Thermal Analysis and Calorimetry 123: 1399-1409.
38. Sarsam WS, Amiri A, Kazi SN, Badarudin A (2016) Stability and Thermophysical Properties of Non-Covalently Functionalized Graphene Nano platelets Nano fluids. Energy Conversion and Management 116: 101-111.
39. Akhavan Zanjani H, Saffar Avval M, Mansourkiaei M, Ahadi M, Sharif F (2014) Turbulent Convective Heat Transfer and Pressure Drop of Graphene-Water Nano fluid Flowing Inside a Horizontal Circular Tube. Journal of Dispersion Science and Technology 35: 1230-1240.
40. Sen Gupta S, Manoj Siva V, Krishnan S, Sreeprasad TS, Singh PK, et al. (2011) Thermal Conductivity Enhancement of Nano fluids Containing Graphene Nano sheets. Journal of Applied Physics 110: 084302.
41. Baby TT, Ramaprabhu S (2010) Investigation of Thermal and Electrical Conductivity of Graphene Based Nano fluids. Journal of Applied Physics 108: 124308.
42. Yu W, Xie H, Chen W (2010) Experimental Investigation On Thermal Conductivity of Nano fluids Containing Graphene Oxide Nano sheets. Journal of Applied Physics 107: 094317.
43. Wang X, Ma Y, Zhu B (2012) State of The Art Ceria-Carbonate Composites (3c) Electrolyte for Advanced Low Temperature Ceramic Fuel Cells (LTCFCs). International Journal of Hydrogen Energy 37: 19417-19425.
44. Malavasi L, Fisher CA, Islam MS (2010) Oxide-Ion and Proton Conducting Electrolyte Materials for Clean Energy Applications: Structural and Mechanistic Features. Chemical Society Reviews 39: 4370-4387.
45. Baiju KV, Shukla S, Biju S, Reddy MLP, Warrier KGK (2009) Hydrothermal Processing of Dye-Adsorbing One-Dimensional Hydrogen Titan ate. Materials Letters 63: 923-926.
46. Xu W, Wang T, Cheng N, Hu Q, Bi Y, eta l. (2015) Experimental and DFT Studies on the Aggregation Behavior of Imidazolium-based surface-active ionic liquids with aromatic counter ions in aqueous solution. Langmuir 31: 1272-1282.
47. Harada M, Cong C (2016) Microwave-Assisted Polyol Synthesis of Polymer-Protected Monometallic Nanoparticles Prepared in Batch and Continuous-Flow Processing. Industrial & Engineering Chemistry Research 55: 5634-5643.
48. Pinto AM, Cabral J, Tanaka DAP, Mendes AM, Magalhães FD (2013) Effect of Incorporation of Graphene Oxide and Graphene Nano platelets On Mechanical and Gas Permeability Properties of Poly (Lactic Acid) Films. Polymer International 62: 33-40.
49. Yiamsawas T, Mahian O, Dalkilic AS, Kaewnai S, Wongwises S (2013) Experimental Studies On the Viscosity of Tio2 and Al2o3 Nanoparticles Suspended in A Mixture of Ethylene Glycol and Water for High Temperature Applications. Applied Energy 111: 40-45.
50. Sun X, Simonsen SC, Norby T, Chatzitakis A (2019) Composite Membranes for High Temperature Pem Fuel Cells and Electrolysers: A Critical Review. Membranes 9: 83.